This is a repository copy of *Exploring the limitations of quantum networking through butterfly-based networks*.

White Rose Research Online URL for this paper:
https://eprints.whiterose.ac.uk/id/eprint/155319/

Version: Accepted Version

Article:

Wilkinson, Kieran N., Cope, Thomas P. W. and Pirandola, Stefano orcid.org/0000-0001-6165-5615 (2020) Exploring the limitations of quantum networking through butterfly-based networks. Advanced Quantum Technologies. 1900103. ISSN: 2511-9044

https://doi.org/10.1002/qute.201900103

Reuse

Items deposited in White Rose Research Online are protected by copyright, with all rights reserved unless indicated otherwise. They may be downloaded and/or printed for private study, or other acts as permitted by national copyright laws. The publisher or other rights holders may allow further reproduction and re-use of the full text version. This is indicated by the licence information on the White Rose Research Online record for the item.

Takedown

If you consider content in White Rose Research Online to be in breach of UK law, please notify us by emailing eprints@whiterose.ac.uk including the URL of the record and the reason for the withdrawal request.

eprints@whiterose.ac.uk
https://eprints.whiterose.ac.uk/

arXiv:1909.02342v3 [quant-ph] 19 Nov 2019

Exploring the limitations of quantum networking through butterfly-based networks

Kieran N. Wilkinson,[1] Thomas P. W. Cope,[2] and Stefano Pirandola[1]
[1] *Computer Science and York Centre for Quantum Technologies, University of York, York YO10 5GH, United Kingdom*
[2] *Department of Mathematics, University of York, York YO10 5DD, United Kingdom*

We investigate the classical and quantum networking regimes of the butterfly network and a group of larger networks constructed with butterfly network blocks. By considering simultaneous multicasts from a set of senders to a set of receivers, we analyze the corresponding rates for transmitting classical and quantum information through the networks. More precisely, we compare achievable rates (i.e., lower bounds) for classical communication with upper bounds for quantum communication, quantifying the performance gap between the rates for networks connected by identity, depolarizing and erasure channels. For each network considered, we observe a range over which the classical rate non-trivially exceeds the quantum capacity. We find that, by adding butterfly blocks in parallel, the difference between transmitted bits and qubits can be increased up to one extra bit per receiver in the case of perfect transmission (identity channels). Our aim is to provide a quantitative analysis of those network configurations which are particularly disadvantageous for quantum networking, when compared to classical communication. By clarifying the performance of these "negative cases", we also provide some guidance on how quantum networks should be built.

I. INTRODUCTION

Bottleneck points arise frequently in network topology. One of the simplest examples of the bottleneck problem is in the butterfly network as shown in Fig. 1. Consider the two-pair communication problem in which the pair of senders A_1 and A_2 perform single-message multicasts to the pair of receivers B_1 and B_2 under the flooding condition that data can only be sent through unused connections. We encounter a bottleneck at node R_1 as data is waiting to be sent from both senders through the channel (R_1, R_2). In 2002, a solution was proposed by Ahlswede et al. in which the bottleneck problem could be bypassed using network coding [1]. As outlined in Fig. 1, network coding in the butterfly network is performed by encoding data using an XOR operation at R_1 and decoding with a second XOR operation at the receivers, after transmission through the bottleneck channel. The result is that each sender successful multicasts their data to both receivers with only a single use of each channel.

In general (and in our work), one may consider the general case where the multicasts can be partially achieved. In fact, in a noisy version of the network, we may associate an average rate to each sender which accounts for the fact that sometimes only a subset of the receivers is reached. In this context we are interested in the average number of bits per receiver that can be transmitted from the senders in each multicast use of the network.

This problem can be analyzed in the setting of quantum information theory [2–9], e.g., connected to the general aim of enabling a wide-spread implementation of a quantum internet [10–16] or to build large communication networks for quantum key distribution [17]. There are several limitations of quantum mechanics that become important in network implementations, most notable the inability to perfectly clone quantum information [18, 19]. It is this property that prevents network coding in the quantum form of the butterfly network. Ref. [20] confirmed that there is no quantum process which achieves network coding with unit fidelity while demonstrating that approximate quantum network coding can be achieved using universal cloning [21], obtaining a fidelity greater than 1/2 but no more than 0.983. Later, Ref. [22] provided an information-theoretic proof that quantum network coding does not provide a larger information flow than routing in the butterfly network.

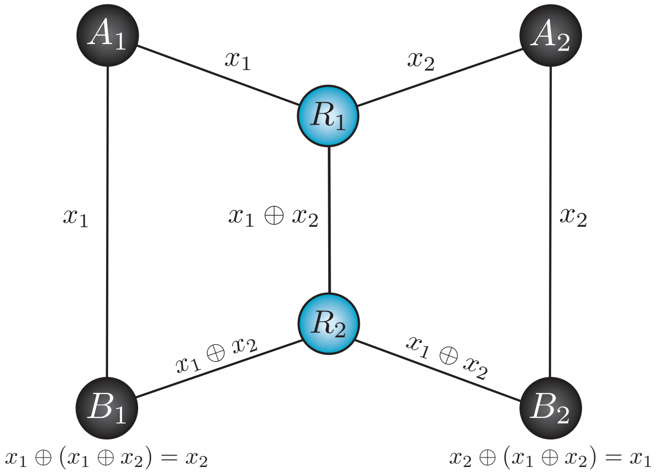

FIG. 1: A schematic of the butterfly network with two senders, A_1 and A_2 and two receivers, B_1 and B_2. A bottleneck channel $R_1 \to R_2$ connects each sender to their indirect receiver. Classical network coding is performed using modulo-2 addition for encoding at R_1 and for decoding B_1 and B_2. Thanks to network coding, both the single-message multicasts $A_1 \to (B_1, B_2)$ and $A_2 \to (B_1, B_2)$ are simultaneously successful.

Perfect quantum network coding has been shown possible in the setting of quantum state transfer in perfect channels. However, achieving this requires the use of additional resources, for example, Ref. [23] showed that perfect network coding can be achieved if the senders share an entangled state before transfer begins. Several other protocols make use of prior entanglement to achieve the same goal [24–26]. Furthermore, a method of quantum computing which utilizes the prior entanglement in the butterfly network to perform unitary operations without the need for further entanglement resources has been developed [27]. Alternatively, Ref. [28] has shown that transfer of quantum states by quantum network coding is possible in the absence of prior entanglement by enabling free classical communication between nodes and several other investigations have considered a free classical communication regime [25, 29–31].

The majority of the literature concerning quantum network coding in the butterfly network has focused on an information processing setting in which quantum states are simply transferred or reconstructed. Here, we consider the problem in a quantum communication setting, in which the quantum systems are physically sent through quantum channels affected by environmental noise. In fact, we investigate the classical and quantum communication rates of the butterfly network based on identity, depolarizing and erasure channels. We build on previous results from Refs. [32–36] to upper bound the highest quantum communication rates achievable in (single-message) multicasts from senders to receivers, assisted by adaptive local operations (LO) and two-way classical communication (CC) involving all the nodes of the network. We then compare these bounds with the corresponding rates that can be achieved for (single-message) multiple multicasts of classical information from senders to receivers, establishing parameter regimes where classical outperforms quantum communication. This analysis is then extended to larger networks built on butterfly network blocks, for which this gap can be amplified. In this way, our study clarifies the nontrivial limitations that certain network architectures have for transmitting quantum information.

II. PRELIMINARY NOTIONS

Before presenting our main results, let us introduce some necessary notions by reviewing some of the theory developed in Refs. [32–36]. These works consider protocols for quantum transmissions, entanglement distribution and secret key generation which are based on the most general LOs assisted by two-way CCs among all the parties involved, that we may briefly call adaptive LOCCs. In particular, Ref. [32] considered point-to-point protocols over a quantum channel, while Ref. [35] extended the study to protocols over repeater chains and, more generally, quantum networks. Finally, Ref. [36] further extended the study to quantum communication networks with multiple senders and receivers.

Using this theory, it is possible to write an upper bound for the total number of qubits that an ensemble of senders can transmit to an ensemble of receivers in terms of the relative entropy of entanglement (REE), defined as

$$E_R(\sigma) = \inf_{\gamma \in \text{sep}} S(\sigma || \gamma) \tag{1}$$

where the infimum is over all the set of separable states (sep) and S is the quantum relative entropy [37]

$$S(\sigma||\gamma) := \text{Tr}\left[\sigma\left(\log_2 \sigma - \log_2 \gamma\right)\right]. \tag{2}$$

In this work we consider the identity, depolarizing and erasure channels, all of which belong to the group of teleportation covariant channels. A channel $\mathcal{E}$ belongs to this group if, for any teleportation unitary U, we may write

$$\mathcal{E}(U\rho U^\dagger) = V\mathcal{E}(\rho)V^\dagger \tag{3}$$

for another (generally different) unitary V. For a teleportation covariant channel $\mathcal{E}$, we may write a single-letter REE bound for its two-way quantum capacity Q_2, i.e. [32]

$$Q_2(\mathcal{E}) \leq E_R(\mathcal{E}) = E_R(\sigma_{\mathcal{E}}) \tag{4}$$

where $E_R(\mathcal{E}) = \max_\sigma E_R\left[(\mathcal{I} \otimes \mathcal{E})(\sigma)\right]$, and $\sigma_{\mathcal{E}} = (\mathcal{I} \otimes \mathcal{E})(\Phi)$ is the Choi matrix of the channel, with Φ being the maximally entangled state. (The proof that the Choi matrix maximizes the REE of a teleportation covariant channel is given in Ref. [32])

In order to generalize these results to teleportation-covariant networks we first introduce some notions from graph theory [34–36]. Let us describe an arbitrary quantum network $\mathcal{N}$ as an undirected graph with nodes or points P and edges E. Two points, x and y, are connected by an edge $(x, y) \in E$ if and only if there is a corresponding quantum channel $\mathcal{E}_{xy}$ between the two. Each point p has a local register of quantum systems over which LOs are performed and optimized on the basis of two-way CCs with the other nodes. Given a set of senders or Alices $\{A_i\}$ and a set of receivers or Bobs $\{B_j\}$, we define a cut C as a bipartition $(\mathbf{A}, \mathbf{B})$ of the points P such that $\{A_i\} \subset \mathbf{A}$ and $\{B_j\} \subset \mathbf{B}$. This is also denoted as $C : \{A_i\}|\{B_j\}$. Then, a cut-set $\tilde{C}$ corresponds to the set of edges (x, y) which are disconnected by the cut C, i.e., such that $x \in \mathbf{A}$ and $y \in \mathbf{B}$.

Let us first consider the unicast configuration where a single sender (Alice, A) communicates with a single receiver (Bob, B) over a quantum network. If the communication is done via a single route, we can obtain an upper bound on the quantum capacity using the single-edge flow of REE through a network. For a cut $C : A|B$ with cutset $\tilde{C}$ and Choi matrix resource state $\sigma_{\mathcal{E}_{xy}}$ for edge $\mathcal{E}_{xy}$, this flow is defined by

$$E_R(C) := \max_{(x,y)\in\tilde{C}} E_R(\sigma_{\mathcal{E}_{xy}}). \tag{5}$$

It can then be shown that the single-path (two-way assisted) quantum capacity of the network is upper-bounded as [35]

$$Q_2(\mathcal{N}) \leq \min_{C:A|B} E_R(C). \tag{6}$$

Alternatively, the parties may choose to use a flooding protocol in which all of the edges of the network are used exactly once by simultaneous routing from Alice to Bob. In this case quantity of interest is the multi-edge flow of REE through cut $C : A|B$ defined by

$$E_R^m(C) = \sum_{(x,y)\in\tilde{C}} E_R(\sigma_{\mathcal{E}_{xy}}) \tag{7}$$

which leads to the following upper bound on the multi-path (two-way assisted) quantum capacity [35]

$$Q_2(\mathcal{N}) \leq \min_{C:A|B} E_R^m(C). \tag{8}$$

The upper bound in Eq. (8) provides the maximum number of qubits that Alice can send to Bob per ‘parallel’ use of the quantum network, where all its edges are simultaneously exploited. Here we note that this upper bound can be modified to bound the total number of qubits that an ensemble of Alices $\{A_i\}$ can send to an ensemble of Bobs $\{B_j\}$. In fact, it is sufficient to consider the two ensembles as super-users and repeat the reasoning, but with the difference that the previous cuts $C : A|B$ must now be replaced by cuts splitting the super-users, i.e., the two ensembles, $C : \{A_i\}|\{B_j\}$. This is an upper bound because the super-users may in principle apply non-local quantum operations among their nodes and, therefore, better optimize the transmission rate with respect to the case of ensembles of separate users. As a result, the optimal rate at which qubits can be transmitted from the senders to the receivers is bounded by

$$\mathcal{B}(\mathcal{N}) := \min_{C:\{A_i\}|\{B_j\}} \sum_{(x,y)\in\tilde{C}} E_R(\sigma_{\mathcal{E}_{xy}}). \tag{9}$$

It is also important to note that this is a general bound for multiple multicasts which applies to both the case of single- and multi-message multicasts from senders to receivers. In fact, since we bound the total number of physical qubits that super Alice transmits to super Bob, it does not matter if these qubits are independent (i.e., in a tensor product of different states) or dependent (e.g., in a global GHZ state [38]) when we unravel super Bob back into an ensemble of Bobs. In this work, we are particularly interested in single-message multiple multicasts, where in each use of the network each Alice aims to send a GHZ-like multipartite logical qubit to the destination set. This is a logical qubit $\alpha|\bar{0}\rangle+\beta|\bar{1}\rangle$ encoded into physical qubits as many as the receivers, i.e., $|\bar{0}\rangle = |0...0\rangle$ and $|\bar{1}\rangle = |1...1\rangle$. In this context, the total number of logical qubits that are correctly received by the destination set is equal to the total number of physical qubits correctly received by each individual receiver, which means that we need to divide the bound in Eq. (9) by the number of receivers r. Therefore our figure of merit is the total number of qubits per use and receiver, which is less than or equal to the quantum bound

$$R_Q(\mathcal{N}) := r^{-1} \min_{C:\{A_i\}|\{B_j\}} \sum_{(x,y)\in\tilde{C}} E_R(\sigma_{\mathcal{E}_{xy}}). \tag{10}$$

III. RATES OF A SINGLE BUTTERFLY BLOCK

By using the bound in Eq. (10), we can see immediately that we cannot obtain more than 1.5 qubits per use and receiver in a butterfly network built with identity channels (for which $E_R(\sigma_{\mathcal{E}_{xy}})$ is equal to one qubit). This comes from the fact that the minimum cut is the middle one disconnecting the edges (A_1, B_1), (R_1, R_2), and (A_2, B_2). This gives 3 physical qubits to be divided by $r = 2$. By contrast, we know from network coding theory that in the classical case we can obtain two classical bits per use and receiver; hence we have a difference of 0.5 bit per use and receiver between the quantum and classical networks in this case.

We can now consider more complicated and realistic cases in which the butterfly network is constructed with noisy channels. Let us start with the depolarizing channel whose action in d dimensions can be expressed as

$$\mathcal{P}_{\text{depol}}(\rho) = (1-p)\rho + \frac{p}{d}\mathcal{I}, \tag{11}$$

where ρ is an arbitrary density matrix and $\mathcal{I}$ is the identity matrix. The action of the channel is to transmit the initial state with probability $1-p$ or a maximally mixed state with probability p (geometrically, the action of the depolarizing channel can be thought of as shrinking the Bloch sphere [3]). At the time of writing the exact two-way quantum capacity of the depolarizing channel is unknown, however Ref. [32] obtained an upper bound of

$$Q_2(p) \leq E_R(\sigma_{\mathcal{P}_{\text{depol}}}) = 1 - H_2\left(1-\frac{3p}{4}\right) \tag{12}$$

for $p \leq 2/3$ with $Q_2 = 0$ otherwise, where $H_2(p) = -p\log_2 p - (1-p)\log_2(1-p)$ is the binary Shannon entropy. Thus, for a butterfly network $\mathcal{B}_{\text{dep}}$ connected by depolarizing channels with equal probability p, the total number of qubits per use and receiver is bounded by

$$R_Q(\mathcal{B}_{\text{dep}}) = \frac{3}{2}\left[1 - H_2\left(1-\frac{3p}{4}\right)\right]. \tag{13}$$

The classical capacities of the depolarizing channel have been extensively studied [40–42]. The unassisted classical capacity is given by

$$C(p) = 1 - H_2\left(1-\frac{p}{2}\right). \tag{14}$$

This can be better understood by propagating an encoded classical bit through the channel. For the input $|0\rangle\langle 0|$, we get

$$\begin{aligned}\mathcal{P}(|0\rangle\langle 0|) &= (1-p)|0\rangle\langle 0| + \frac{p}{2}(|0\rangle\langle 0| + |1\rangle\langle 1|)\\ &= \left(1-\frac{p}{2}\right)|0\rangle\langle 0| + \frac{p}{2}|1\rangle\langle 1|,\end{aligned} \tag{15}$$

similarly for $|1\rangle\langle 1|$,

$$\mathcal{P}(|1\rangle\langle 1|) = \left(1-\frac{p}{2}\right)|1\rangle\langle 1| + \frac{p}{2}|0\rangle\langle 0|. \tag{16}$$

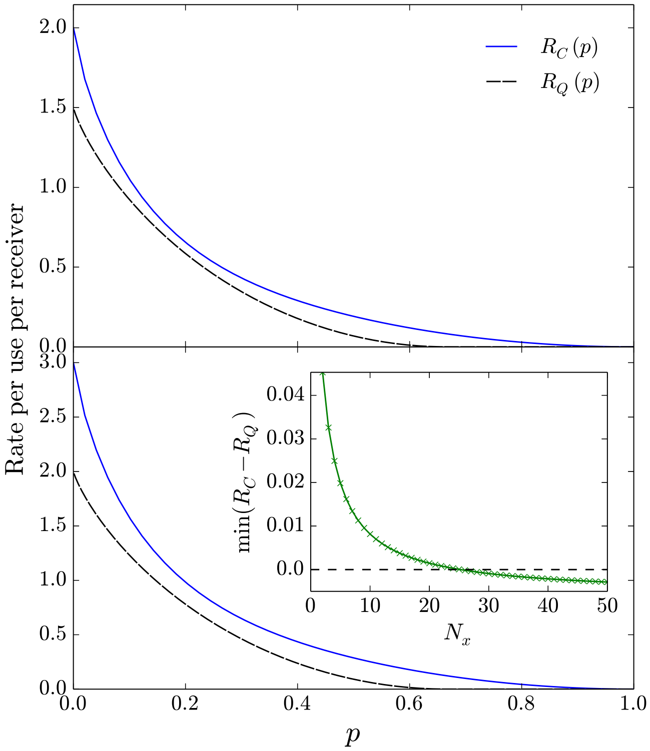

FIG. 2: Rates (bits/qubits) per use and receiver for the depolarizing case considering a single butterfly block (upper panel) and the limit of $N_x \to \infty$ blocks in parallel (lower panel). We plot the achievable classical rate R_C (solid blue line) and the quantum bound R_Q (dashed black line). The inset shows the minimum difference between the classical rate and the quantum bound as a function of N_x (where the minimization is taken over the probabilities).

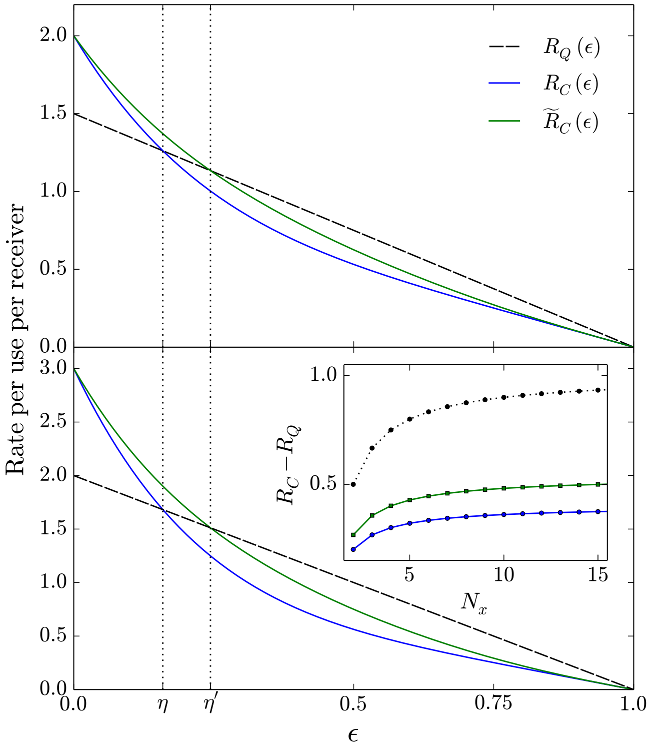

FIG. 3: Rates (bits/qubits) per use and receiver for the erasure case, considering a single butterfly block (upper panel) and the limit of $N_x \to \infty$ blocks in parallel (lower panel). We plot the quantum bound R_Q (dashed black line), the achievable classical rate R_C (solid blue line) and the inter-node-assisted achievable classical rate $\tilde{R}_C$ (solid green line). Note that the maximum gap is achieved for $\epsilon = 0$ where the channels become identity channels. At that point, for a single butterfly block, we find the expected result of 2 bits versus 1.5 qubits per use per receiver. In the figure, η and η' are the critical points at which R_C and $\tilde{R}_C$, respectively cross the quantum bound R_Q. Inset: Difference between $\tilde{R}_C$ and R_Q as a function of N_x for values of erasure probability equal to 0 (black line) and $\eta'/2$ (green line), and the difference between R_C and R_Q as a function of N_x for erasure probability equal to $\eta/2$ (blue line).

What we have is the equivalent of a classical binary symmetric channel (BSC) with bit flip probability $p/2$ [39].

To compute an achievable rate for the classical single-message multiple multicast over a depolarizing/BSC butterfly network, we deconstruct the network in the two channels $A_1, A_2 \to B_1$ and $A_1, A_2 \to B_2$. Calculating the total rate of the combined channels gives an achievable rate for the network. The general procedure for this process is to create the transition probability matrix using the logic of the butterfly network, followed by an optimization over a distribution on the input symbol. The upper panel of Fig. 2 shows both the quantum bound R_Q (qubits per per use and receiver) and the achievable rate R_C for sending classical information (bits per use and receiver). The quantum bound is exceeded by the classical rate over the entire range of p with the maximum difference being 0.5 bits per receiver (which corresponds to the ideal case of identity channels discussed above).

Let us now move on to erasure channels. From classical information theory we know that the capacity of the binary erasure channel with erasure probability ϵ is given by $C(\epsilon) = 1 - \epsilon$. This formula has also been shown to be equal to the classical capacity of the quantum erasure channel [43]. The same work found the quantum capacity to be $Q(\epsilon) = \max\{0, 1 - 2\epsilon\}$ and also $C(\epsilon) = Q_2(\epsilon) = 1 - \epsilon$. The erasure channel is unique in that the number of correctly transmitted bits is known with certainty, so that the capacity is equivalent to the average number of transmitted bits. For any network it is straightforward to calculate the achievable classical rate. For a single butterfly network block $\mathcal{B}_{\text{era}}$ connected by erasure channels with the same probability, we obtain the classical rate (per use and receiver)

$$R_C(\mathcal{B}_{\text{era}}) = (1 - \epsilon) + (1 - \epsilon)^5, \tag{17}$$

where the first term arises from the contribution of the side channels, and the second comes from network coding at the bottleneck node.

Allowing side one-way CC between nodes in the network allows for the optimization of the transmission routes, increasing the rate. For example, if we detect a failure in a channel connected to the bottleneck node, (A_i, R_1), we send any data received at R_1 directly to R_2 and subsequently to both receivers. We then have additional communication paths from A_j to B_i and B_j. The inter-node-assisted rate (per use and receiver) is given by

$$\tilde{R}_C(\mathcal{B}_{\mathrm{era}}) = (1-\epsilon) + (1-\epsilon)^5 + \epsilon(1+\epsilon)(1-\epsilon)^3. \quad (18)$$

The upper panel of Fig. 3 shows each of the rates for a single butterfly block. For both R_C and $\tilde{R}_C$, we observe a region where the quantum bound R_Q is exceeded. We label the crossing points $\eta = 0.159$ and $\eta' = 0.244$ for R_C and $\tilde{R}_C$, respectively. The advantage of inter-node classical communications is significant, and extends the performance difference between the classical and quantum butterfly network in this configuration.

IV. BUILDING NETWORKS WITH BUTTERFLY BLOCKS

We will now expand our analysis to larger networks constructed with butterfly network blocks as shown in Fig. 4. We consider adding blocks in parallel in Sec. IV A, in series in Sec. IV B and in both series and parallel in Sec. IV C.

A. Butterfly blocks connected in parallel

Firstly, we consider the case in which we have a single row of N_x connected butterfly blocks, such that we have a network $\mathcal{N}_{\mathrm{par}}$ with $r = N_x + 1$ senders/receivers. We extend the previous reasoning to evaluate the maximum number of multipartite logical qubits that can be flooded/transmitted from senders to receivers per use of the network. This is equal to the total number of physical qubits transmitted per use and receiver, for which we can write corresponding upper bounds. In particular, for the depolarizing case, we have the quantum bound

$$R_Q = \frac{2r-1}{r}\left[1 - H_2\left(\frac{3p}{4}\right)\right], \quad (19)$$

while for the erasure case we write

$$R_Q = \frac{2r-1}{r}(1-\epsilon). \quad (20)$$

The achievable rate of the depolarizing network can be found by expanding the methods used for the single butterfly block case. The network can be deconstructed into two channels of the form $A_i, A_{i+1} \to B_i$ at the ends of the network, and $(N_x - 1)$ channels of the form $A_i, A_{i+1}, A_{i+2} \to B_{i+1}$. We find the overall rate numerically from the combination of the capacities of all channels, from which we can compute the rate per user and receiver R_C. For the erasure case we can directly write the following rate per user and receiver

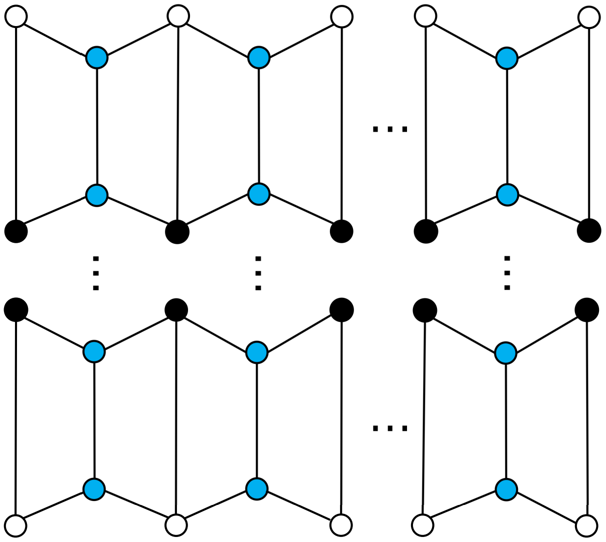

FIG. 4: Diagram of the construction of larger networks from butterfly network blocks in parallel (horizontal) and series (vertical).

$$R_C = (1-\epsilon) + \frac{2(r-1)}{r}(1-\epsilon)^5. \quad (21)$$

Here the first term on the right hand side is due to the fact that all receivers may receive a single bit from their directly connected sender, while the second term accounts for the fact that all receivers (except the extremal ones B_1 and B_r) may receive two bits from successful network coding on the adjacent intermediate nodes. In the case of inter-node CC, the rate can be generalized by recognizing that we have Eq. (21) plus four backup routes per butterfly block, giving an overall rate of

$$\tilde{R}_C = (1-\epsilon) + \frac{2(r-1)}{r}\left[(1-\epsilon)^5 + \epsilon(1+\epsilon)(1-\epsilon)^3\right]. \quad (22)$$

We see immediately for the erasure network that the difference between the average number of bits/qubits grows monotonically as we increase the number of butterfly blocks. Taking the limit of large r for the rates of the erasure case we obtain

$$\lim_{r\to\infty} R_Q = 2(1-\epsilon) \quad (23)$$

$$\lim_{r\to\infty} R_C = (1-\epsilon) + 2(1-\epsilon)^5 \quad (24)$$

$$\lim_{r\to\infty} \tilde{R}_C = (1-\epsilon) + 2(1-\epsilon)^5 + 2\epsilon(1+\epsilon)(1-\epsilon)^3. \quad (25)$$

The lower panel of Fig. 2 shows the rates of the depolarizing case in the limit of large r for the entire range of probabilities. The asymptotic rates are approximately identical at 0.2 but the classical case outperforms the quantum bound everywhere else in the range. The lower panel of Fig. 3 shows the asymptotic rates for the erasure case. We find that η and η' are equivalent to the single block case for any non-zero N_x. At small values of the erasure probability ϵ, the gap between the rates tends to one bit per use per receiver.

B. Butterfly blocks connected in series

We now consider the rates of a network $\mathcal{N}_{\rm ser}$ consisting of N_y butterfly network blocks connected in series i.e. in a ladder formation. The number of receivers is the same ($r = 2$) but the number of intermediate nodes and channels has increased. The addition of extra blocks has the effect of reducing the rates, as it becomes harder to reach a receiver without the incurrence of errors.

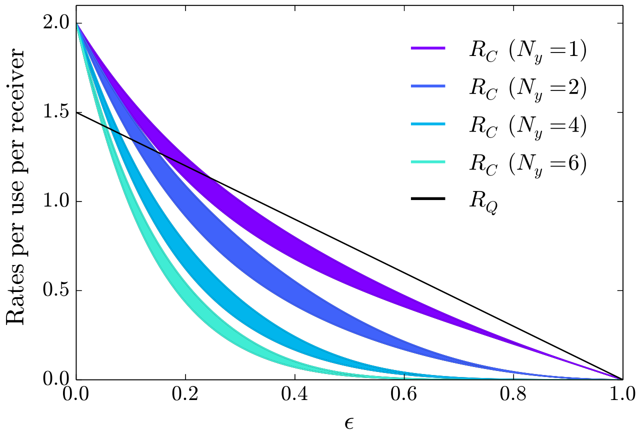

FIG. 5: Classical rate (lower lines) and inter-node CC assisted classical rate (upper lines) per receiver for a $1 \times N_y$ butterfly block network constructed with erasure channels. Comparison with the quantum bound (solid black line).

For the depolarizing case, adding blocks in a ladder structure is equivalent to adding only extra side channels above a single block. However, in the erasure case, extra bottlenecks can be used effectively, even if there are no additional communications. If we allow the nodes to duplicate data, we can use the bottleneck channels as effective backup channels in case of errors and perform network coding in the final bottleneck before the receivers.

Let us firstly consider only two blocks in series. We have the option to ignore the bottleneck structure in the first block entirely and send only via the side quantum channels. In this case the classical rate (per use and receiver) is given by

$$R_C = (1-\epsilon)^2 + (1-\epsilon)^7 \tag{26}$$

which is however not optimal. A more effective strategy is to use the bottleneck as an effective backup channel, by sending a bit from A_1 to the intermediate node on A_1's side of the network, which we briefly label I_1, via the channel $R_1 \to R_2$ as well as through the direct channel $A_1 \to I_1$. Now I_1 has a greater probability of receiving the correct bit, and because there are no additional operations, no communication between nodes is required. We can calculate the probability that a correct bit is received by computing

$$\lambda = 1 - P(\text{fail}) = 1 - \epsilon[1-(1-\epsilon)^3] \tag{27}$$

and the classical rate (per use and receiver) is therefore given by

$$R_C = \frac{(1-\epsilon)\lambda + (1-\epsilon)^2}{2} + (1-\epsilon)^6\lambda. \tag{28}$$

There is no further way we can improve the rate without the receivers losing certainty of what has been sent.

This strategy can be extended to any number of blocks in series, where a backup channel can be applied once per block. Sender/intermediate nodes on either side of the network can use the bottleneck route, however, for more than two blocks the rate is maximized when the routes are always used by nodes on the same side of the network. The previous classical rate can be generalized as

$$R_C = \frac{(1-\epsilon)\lambda^{N_y-1} + (1-\epsilon)^{N_y}}{2} + (1-\epsilon)^5(1-\epsilon)^{N_y-1}\lambda^{N_y-1}. \tag{29}$$

Alternatively, if we allow inter-node communication, the classical rate of a $1 \times N_y$ erasure network is obtained by considering all of the possible paths from sender to receiver, while prioritizing the backup route in upper blocks, and accounting for possible channel failures. The classical rates for the $1 \times N_y$ network are shown in Fig. 5 and compared with the quantum bound R_Q which does not depend on N_y. Clearly the value of the crossing point η' decreases rapidly as N_y increases, but there is still a significant gap between the upper bound on the quantum rate and the achievable classical rate.

C. Butterfly blocks connected in series and parallel

Finally, we come to the most complex case in which we consider a general $N_x \times N_y$ grid of butterfly network blocks. This means that we have $r = N_x + 1$ receivers. Again, we calculate the classical rates, accounting for how the additional bottlenecks may be exploited. By allowing each sender (excluding the one at the right edge of the network) to use the backup route to the its right in $(N_y - 1)$ upper blocks, we obtain the following unassisted classical rate (per use and receiver) for a general grid

$$\begin{aligned} R_C = \frac{1}{N_x+1}\{&N_x(1-\epsilon)\lambda^{N_y-1} + (1-\epsilon)^{N_y} \\ &+ 2(N_x-1)(1-\epsilon)^5\lambda^{2(N_x-1)} \\ &+ 2(1-\epsilon)^5(1-\epsilon)^{N_y-1}\lambda^{N_y-1}\}. \end{aligned} \tag{30}$$

For the inter-node assisted rate, we repeat the strategy of the series-only case and obtain values of η' for different configurations. The top panel of Fig. 6 shows the relative increase in the critical point η' with respect to the series-only case. The increase is significant and increases with the number of blocks we have in series. The lower panel shows η' as a function of N_y. The point η' decreases rapidly as we increase the number of blocks between sender and receiver, however the results show that we always have a finite range over which the classical rate exceeds the quantum bound. These results demonstrate that by adding more blocks in parallel we can increase η' up to a convergence point, increasing by more than 60% in some cases.

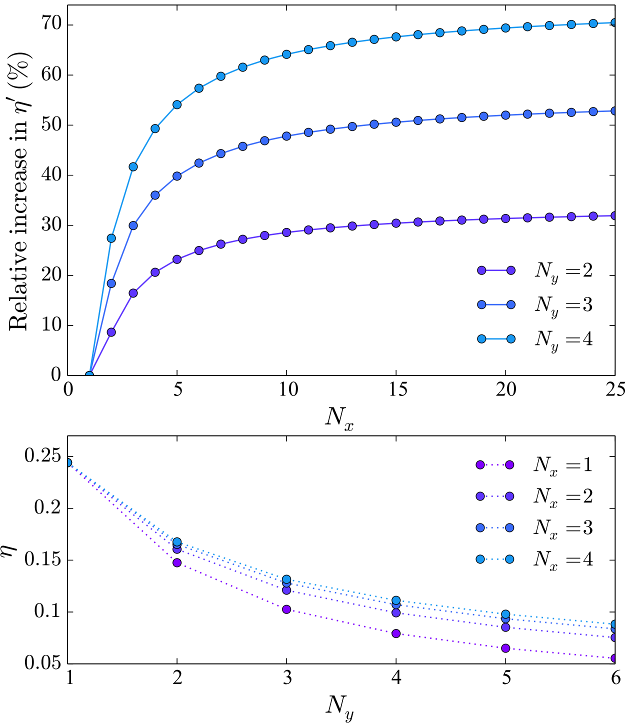

FIG. 6: Upper panel: relative increase in the critical point η' as compared to the $N_x = 1$ case for various values of N_y. Lower panel: variation of η' with N_y for various values of N_x.

V. CONCLUSIONS

Our results show that, when we consider single-message multiple multicasts over a quantum network constructed with butterfly network blocks, there is an important discrepancy between quantum and classical communication rates. We have demonstrated that this discrepancy can be monotonically increased by adding additional blocks in parallel, up to a maximum value of one bit/qubit per use and receiver for networks constructed using identical erasure channels.

By exploiting inter-node classical communication in erasure networks, we have shown that the discrepancy is increased more rapidly. Additionally, in this case we observe a notable discrepancy even when we add blocks in series and the number of butterfly blocks separating senders from receivers is large. By adding further blocks in parallel to create a grid, we can increase the discrepancy by more than 60%, i.e., in the value of the critical point at which the classical rate beats the quantum bound.

Our results demonstrate that duplicating certain existing classical network structures containing butterfly blocks in order to build quantum counterparts can result in significantly lower performance. It may be possible to exploit this performance discrepancy in order to create a system in which a quantum communication cannot beat a classical equivalent. In this sense, our results provide a theoretical guide with which to engineer such a system.

Acknowledgments. This work has been supported by the EPSRC via the “UK Quantum Communications HUB” (EP/M013472/1) and by the European Union via the project “Continuous Variable Quantum Communications” (CiViQ, no 820466).

[1] Ahlswede, R and N. Cai, S.-Y. Li, and R. W. Yeung, IEEE Trans. Inf. Theory, **46**, 1204, (2000).
[2] J. Watrous, *The theory of quantum information* (Cambridge University Press, Cambridge, 2018).
[3] M. A. Nielsen, Michael and I. Chuang, *Quantum computation and quantum information* (2002).
[4] J. Preskill, *Lecture notes for physics 229: Quantum information and computation* (1998)
[5] I. Bengtsson and K. Życzkowski, *Geometry of quantum states: An Introduction to Quantum Entanglement* (Cambridge University Press, Cambridge 2006).
[6] A. Holevo, *Quantum systems, channels, information: A mathematical introduction* (De Gruyter, Berlin-Boston, 2012).
[7] S. L. Braunstein, and P. Van Loock, Rev. Mod. Phys. **77**, 513 (2005).
[8] C. Weedbrook, S. Pirandola, R. García-Patrón, N. J. Cerf, T. C. Ralph, J. H. Shapiro, and S. Lloyd, Rev. Mod. Phys. **84,** 621-699 (2012).
[9] U. L. Andersen, J. S. Neergaard-Nielsen, P. van Loock, and A. Furusawa, Nat. Phys. **11**, 713–719 (2015).
[10] H. -J. Briegel, W. Dür, J. I. Cirac, and P. Zoller, Phys. Rev. Lett. **81**, 5932 (1998).
[11] W. Dür, H.-J. Briegel, J. I. Cirac, and P. Zoller, Phys. Rev. A **59**, 169 (1999).
[12] L. -M. Duan, M. D. Lukin, J. I. Cirac, and P. Zoller, Nature **414**, 413 (2001).
[13] H. J. Kimble, Nature **453**, 1023 (2008).
[14] R. Van Meter, “Quantum Networking”, John Wiley & Sons, Wiley (2014).
[15] S. Pirandola, J. Eisert, C. Weedbrook, A. Furusawa, and S. L. Braunstein, Nature Photonics **9**, 641-652 (2015).

[16] S. Pirandola and S. L. Braunstein, Nature **532**, 169 (2016).

[17] S. Pirandola, U. L. Andersen, L. Banchi, M. Berta, D. Bunandar, R. Colbeck, D. Englund, T. Gehring, C. Lupo, C. Ottaviani, J. Pereira, M. Razavi, J. S. Shaari, M. Tomamichel, V. C. Usenko, G. Vallone, P. Villoresi, and P. Wallden, *Advances in Quantum Cryptography*, preprint arXiv:1906.01645 (2019).

[18] J. Park, Foundations of Physics. **1**, 23-33 (1970).

[19] W. K. Wootters and W. H. Zurek, Nature **299**, 802 (1982).

[20] M. Hayashi, K. Iwama, H. Nishimura, R. Raymond. and S. Yamashita, in STACS (2007), pp. 610–621.

[21] V. Bužek and M. Hillery, Phys. Rev. A **54**, 1844 (1996).

[22] A. Jain, M. Franceschetti, and D. A. Meyer, J. Math. Phys. **52**, 032201 (2011).

[23] M. Hayashi, Phys. Rev. A **76**, 040301 (2007).

[24] T. Satoh, F. Le Gall, and H. Imai, Phys. Rev. A **86**, 032331 (2012).

[25] H. Nishimura, in International Symposium on Network Coding (NetCod) (2013), pp. 1-5.

[26] Z.-Z. Li, G. Xu, X.-B. Chen, Z. Qu, X.-X. Niu, and Y.-X. Yang, Sci. China Inf. Sci. **62**, 12501 (2019).

[27] A. Soeda, Y. Kinjo, P. S. Turner, and M. Murao, Phys. Rev. A **84**, 012333 (2011).

[28] H. Kobayashi, F. Le Gall, H. Nishimura, and M. Rötteler, in Automata, Languages and Programming (2009), pp. 622–633.

[29] H. Kobayashi, F. Le Gall, H. Nishimura, and M. Rötteler, in IEEE International Symposium on Information Theory (2011), pp. 109–113.

[30] D. Leung, J. Oppenheim, and A. Winter, IEEE Trans. Inf. Theory **56** 3478 (2010).

[31] M.-X. Luo, G. Xu, X.-B. Chen, Y.-X. Yang, and X. Wang, Sci. Rep. **4**, 4571 (2014).

[32] S. Pirandola, R. Laurenza, Riccardo, C. Ottaviani, and L. Banchi, Nat. Commun. **8**, 15043 (2017). See also preprint arXiv:1510.08863 (2015).

[33] S. Pirandola, S. L. Braunstein, R. Laurenza, C. Ottaviani, T. P. W. Cope, G. Spedalieri, and L. Banchi, Quantum Sci. Technol. **3**, 035009 (2018).

[34] S. Pirandola, *Capacities of repeater-assisted quantum communications*, preprint arXiv:1601.00966 (2016).

[35] S. Pirandola, Commun. Phys. **2**, 51 (2019).

[36] S. Pirandola, Quantum Sci. Technol. **4**, 045006 (2019).

[37] V. Vedral, Rev. Mod. Phys. **74**, 197 (2002).

[38] D. M. Greenberger, M. A. Horne, and Anton Zeilinger, *Bell's theorem, Quantum Theory, and Conceptions of the Universe* (Kluwer Academics, Dordrecht, The Netherlands 1989), pp. 73-76.

[39] T. M. Cover and J. A. Thomas, *Elements of Information Theory* (2nd edn, New York, Wiley, 2006).

[40] J. Mulherkar, Int. J. Quantum Inform. **14**, 1650017 (2016).

[41] J. Wouters, M. Fannes, I. Akhalwaya, and F. Petruccione, Phys. Rev. A **79**, 042303 (2009).

[42] C. King, IEEE Trans. Inf. Theory **49**, 221 (2003).

[43] C. H. Bennett, D. P. DiVincenzo and J. A. Smolin, Phys. Rev. Lett. **78**, 3217 (1997).